0090-9556/08/3607-1322–1331$20.00
DRUG METABOLISM AND DISPOSITION
Vol. 36, No. 7
21261/3354389
DMD 36:1322–1331, 2008
Printed in U.S.A.

Functional Expression and Comparative Characterization of Nine Murine Cytochromes P450 by Fluorescent Inhibition Screening[S]

Lesley A. McLaughlin, Leslie J. Dickmann,[1] C. Roland Wolf, and Colin J. Henderson

Cancer Research UK, Molecular Pharmacology Unit, Biomedical Research Centre, University of Dundee, Ninewells Hospital and Medical School, Dundee, United Kingdom

Received March 3, 2008; accepted April 16, 2008

ABSTRACT:

The increasing number of transgenic or gene knockout mouse models generated for use in drug metabolism studies has meant that a greater understanding of the function and substrate specificities of murine cytochromes P450 (P450s) has become essential, particularly with the recent advances in "humanized" mouse models. In this study, we have heterologously expressed nine murine P450s—Cyp1a1, Cyp1a2, Cyp1b1, Cyp2a4, Cyp2b20, Cyp2c29, Cyp2d22, Cyp2e1, and Cyp3a11—individually with human P450 oxidoreductase to generate functional monooxygenase systems in *Escherichia coli*. We have identified a suitable fluorogenic probe for each P450 and determined the apparent kinetic parameters. These probes have enabled the screening of a panel of 31 test compounds classified as "drugs," "natural compounds," "endogenous compounds," and "pesticides" by measurement of IC_{50}, thus allowing the comparison of binding affinities. Human P450s CYP2C9, CYP2D6, and CYP3A4 were also included in the study to enable direct comparisons to be made with the mouse enzymes. Although there were general similarities between human and mouse P450s, perhaps the most significant finding in this study was the observation that, despite 77% amino acid identity, Cyp2d22 and CYP2D6 were remarkably dissimilar in a range of enzymatic properties, with potentially serious implications for pharmacokinetic studies using CYP2D substrates. The data presented in this study provide a solid foundation with which to assess the degree of similarity (or difference) between mouse and human P450s involved in xenobiotic metabolism and can be used as a basis for further studies.

The cytochromes P450 are a superfamily of heme-containing monooxygenases that play a pivotal role in endogenous metabolic pathways including steroid, fatty acid, bile acid, and prostaglandin biosynthesis (Miller, 1988; Hasler, 1999), and they are also responsible for the detoxification of a vast array of xenobiotics, including environmental pollutants and the majority of small molecule therapeutic drugs (Guengerich, 2005). In addition, P450s have also been implicated as having critical functions during embryogenesis (Abu-Abed et al., 2001; Otto et al., 2003). These enzymes are ubiquitously expressed in virtually all murine tissues, and, to date, 103 full-length P450 genes and 88 pseudogenes have been identified in the *Mus musculus* genome (http://drnelson.utmem.edu/cytochromeP450.html); however, the functions and substrate specificities of the majority of these enzymes are as yet undefined.

Several murine P450 knockout models have been generated, as well as a conditional deletion of hepatic NADPH-cytochrome P450 reductase (POR) (Henderson et al., 2003; Henderson and Wolf, 2003; Wu et al., 2003), the redox partner of microsomal P450s, which have proved to be invaluable for the study of P450 functions in vivo. In general terms, these experiments demonstrated that ablation of a P450 gene that is involved in a vital endogenous pathway (e.g., the cholesterol 7α hydroxylase, Cyp7a1) lead to either embryonic or perinatal lethality (Ishibashi et al., 1996), whereas knockout of a purely xenobiotic metabolizing enzyme (e.g., Cyp1a1) caused little difference in phenotype until a chemical challenge occurred (Dalton et al., 2000; Henderson and Wolf, 2003). Further investigation using transgenic animal models coupled with classical biochemical analysis has shed some light on the preferred substrates of some of the more conserved murine xenobiotic metabolizing P450s. The complication of multiplicity in several P450 families makes it extremely difficult to identify the in vivo function of any one particular enzyme. For example, the mouse Cyp2c, -2d, and Cyp3a subfamilies have 15, 9, and 8 members, respectively.

Of particular interest are murine Cyp1a1, Cyp1a2, Cyp1b1, Cyp2a4, Cyp2b20, Cyp2c29, Cyp2d22, Cyp2e1, and Cyp3a11. These isoforms are either orthologs of, or are closely related to (by phylogeny and expression patterns), the key human xenobiotic metabolizing P450s (Table 1; Supplemental Data). Since the substrate specificities of the human enzymes have been investigated in detail, the same types

C.R.W. is funded by a Programme Grant Award from Cancer Research UK.

[1] Current affiliation: Biochemistry and Biophysics Group, Pharmacokinetics and Drug Metabolism, Amgen, Inc., Seattle, WA.

Article, publication date, and citation information can be found at http://dmd.aspetjournals.org.

doi:10.1124/dmd.108.021261.

[S] The online version of this article (available at http://dmd.aspetjournals.org) contains supplemental material.

ABBREVIATIONS: P450, cytochrome P450; AMMC, 3-[2-(*N*,*N*-diethyl-*N*-methylammonium)-ethyl]-7-methoxy-4-methylcoumarin; BFC, 7-benzyloxy-4-trifluoromethylcoumarin; BQ, 7-benzyloxyquinoline; BR, benzyloxyresorufin; cc, correlation coefficient; ER, ethoxyresorufin; DBF, dibenzyl fluorescein; MFC, 7-methoxy-4-trifluoromethylcoumarin; MR, methoxyresorufin; POR, P450 oxidoreductase; PR, pentoxyresorufin; RT-PCR, reverse transcriptase-polymerase chain reaction; CHAPS, 3-[(3-cholamidopropyl)dimethylammonio]-1-propanesulfonic acid.

TABLE 1

Oligonucleotides used to generate P450 cDNAs and bacterial expression constructs

P450	Oligo[a]	Sequence
Cyp1a1	RT-PCR (fp)	ATGCCTTCCATGTATGGACTTCC
Cyp1a1	RT-PCR (rp)	CTAAGCCTGAAGATGCTGAGGACC
Cyp2b20	RT-PCR (fp)	GTCAGCCACCATGGAGCCCAGTGTGCTGCTCC
Cyp2b20	RT-PCR (rp)[b]	CGCGAATTCCTACAGATCTTCTTCAGAAATAAGTTTTTGTTCGCGGGCCAAGAAGCAGATCTGG
OmpA	OmpA (fp) NdeI site	GGAATTCCATATGAAAAAGACAGCTAT
OmpA	OmpA (fp) BamHI site	GGGGATCCCATATGAAAAAGACAGCTAT
Cyp1a1	OmpA fusion primer (rp)	GGCTGACACGAAGGCTGGAAGTCCATACATGGAAGCCATCGGAGCGGCCTGCGCTACGGTAGCGAA
Cyp1a1	His_6 tag (rp) (EcoRI site)	CGGGAATTCCTAGTGATGGTGATGGTGATGAGCCTGAAGATGCTGAGGACCAGAAGACCG
Cyp1a2	OmpA fusion primer (rp)	TAAGGAGATGTACTGGGAGAACGCCATCGGAGCGGCCTGCGCTACGGTAGCGAA
Cyp1a2	His_6 tag (rp) (KpnI site)	CGGGGTACCTCAATGGTGATGGTGATGGTGCTTGGAAAAGCGTGGCCATGCCTGG
Cyp1b1	OmpA fusion primer (rp)	GTCTGCACTAAGGCTGGTGGCCATCGGAGCGGCCTGCGCTACGGTAGCGAA
Cyp1b1	His_6 tag (rp) (EcoRI site)	GCCCGAATTCAGTGATGGTGATGGTGATGCTTGCAGCCTTCCTCAGTTTGCAG
Cyp2a4	From ATG (fp)	ATGCTGACCTCAGGACTC
Cyp2a4	His_6 tag (rp) (HinDIII site)	CCCCAGGCTTTCAATGGTGATGGTGATGGTGACGGGACAAGAAACTCATAGT
Cyp2b20	OmpA fusion primer	GAGAGCAAGGAGGAGCAGCACACTGGGCGCCATCGGAGCGGCCTGCGCTACGGTAGCGAA
Cyp2b20	His_6 tag (rp) (EcoRI site)	CCGGAATTCTCAGTGATGGTGATGGTGATGGCGGGCCAAGAAGCAGATCTGGTA
Cyp2c29	OmpA fusion primer (rp)	GAGCGCTAGGAACACGACCAGCGCCATCGGAGCGGCCTGCGCTACGGTAGCGAA
Cyp2c29	His_6 tag (rp) (EcoRI site)	CGGAATTCTTAGTGATGGTGATGGTGATGGAGAGGAATGAAGCAGAGCTGGT
Cyp2d22	OmpA fusion primer (rp)	GCCCCGGTCGGCAGTCTCATCGGAGCGGCCTGCGCTACGGTAGCGGAA
Cyp2d22	(rp) (EcoRI site)	CGGGAATTCTTAGCGGGGCAAAGCACAGAG
Cyp2e1	OmpA fusion primer (rp)	GGCAACGGTGATGCCAAGAACCGCCATCGGAGCGGCCTGCGCTACGGTAGCGAA
Cyp2e1	His_6 tag (rp) (HinDIII site)	CCCCAGGCTTTCAATGGTGATGGTGATGGTGTGAACGAGGAATGACACAGAG
Cyp3a11	OmpA fusion primer (rp)	CAGTGAGAGAGCTGAAACCAGGGCCATCGGAGCGGCCTGCGCTACGGTAGCGAA
Cyp3a11	His_6 tag (rp) (Kpn I site)	CGGGGTACCTCAGTGATGGTGATGGTGATGTGCTCCAGTTATGACTGCATCCCG

fp, forward primer; rp, reverse primer.
[a] Oligos are described in 5′ to 3′ direction.
[b] Primer also contains c-Myc epitope tag for other unrelated work.

of chemical compounds have been used to screen the murine enzymes. The majority of work has focused on Cyp1a1, Cyp1a2, Cyp1b1, and Cyp2e1, which are reasonably well conserved between species and have also been knocked out in mouse models available for in vivo studies (Pineau et al., 1995; Lee et al., 1996; Buters et al., 1999; Dalton et al., 2000). The known substrates of these particular enzymes (Table 1; Supplemental Data) tally well with the data for the human orthologs (Guengerich, 2005), indicating similar substrate specificities. However, it is difficult to find data in the literature that compare metabolic profiles or ligand binding of particular compounds with what is considered to be equivalent murine and human P450.

In response to this, we have heterologously coexpressed a panel of nine murine P450s with human POR in *Escherichia coli*, thus creating functional monooxygenase systems for enzyme characterization. For each P450, we have identified a fluorogenic probe substrate and determined the apparent kinetic parameters. These probe substrates were then used to determine the IC_{50} of 31 test compounds for each murine enzyme, allowing us to compare inhibitory potencies. Furthermore, we have screened human CYP2C9, CYP2D6, and CYP3A4 with the same panel of test compounds, allowing direct comparison of inhibitory potencies between human and mouse enzymes.

Materials and Methods

Reagents. All chemicals, unless otherwise stated, were purchased from Sigma-Aldrich (Poole, UK) or Fluka (Gillingham, UK). Ampicillin was obtained from Beecham Research (Welwyn, Garden City, UK) and isopropyl β-D-thiogalactopyranoside and δ-aminolevulinic acid were from Melford Laboratories (Ipswich, UK). Competent *E. coli* JM109 and DH5α cells were purchased from Promega (Southampton, UK) and Invitrogen (Paisley, UK). 3-[2-(*N*,*N*-Diethyl-*N*-methylammonium)-ethyl]-7-methoxy-4-methylcoumarin (AMMC), dibenzyl fluorescein (DBF), 7-methoxy-4-trifluoromethylcoumarin (MFC), 7-benzyloxyquinoline (BQ), and 7-benzyloxy-4-trifluoromethylcoumarin (BFC) were purchased from BD Gentest (Cowley, UK), whereas VIVID CYP2D6 Cyan, VIVID 3A4 Red, VIVID 2C9 Red, and VIVID 3A4 Green were from Invitrogen.

cDNA Clones. Where available, the mouse P450 cDNA clones were purchased as I.M.A.G.E. clones from MRC Geneservice (Cambridge, UK). Cyp1a1 and Cyp2b20 cDNAs were generated by RT-PCR from 3-methylcholanthrene-induced mouse liver RNA using Superscript 1st Strand Synthesis Kit (Invitrogen) to perform the reverse transcription [oligo(dT) primer] and Pfu DNA polymerase (Promega) to isolate the specific full-length cDNA clones. Details of oligonucleotides used are shown in Table 1. The isolated cDNAs were cloned into pCR-Blunt (Promega) and sequenced to confirm identity.

Bacterial Expression Constructs. cDNAs, with the exception of Cyp2d22 and Cyp2a4, were modified at the 5′ end by mutating position +2 to alanine, and fusion by PCR to a bacterial OmpA (+2) leader sequence using an OmpA forward primer containing either an NdeI or BamHI restriction site, a reverse OmpA-cDNA fusion primer, and a reverse primer containing the 3′ end of the cDNA, His_6-tag, and a unique restriction site. The oligos used are listed in Table 2. PCR was performed as previously described (Pritchard et al., 1997; Pritchard et al., 1998). Modified cDNAs were cloned into pB13, a modified version of pCW (Pritchard et al., 1997), using the appropriate restriction sites. Cyp2d22 was modified essentially as described, but without the His_6-tag. Cyp2a4 was cloned as full-length His_6-tagged PCR product into pB13, which had been modified to contain the OmpA sequence. All constructs were confirmed by DNA sequencing. The plasmids used to express CYP2C9, -2D6, and -3A4 have been previously described (Pritchard et al., 1997; Pritchard et al., 1998; Flanagan et al., 2003).

Heterologous Coexpression in *E. coli*. Competent *E. coli* JM109 or DH5α cells were cotransformed with an individual P450 and pJR7, a plasmid which expresses human POR (Blake et al., 1996; Pritchard et al., 1997; Pritchard et al., 1998). Bacterial expression, membrane isolation, and determination of P450 content were carried out as previously described (Pritchard et al., 1998). The rate of reduction of cytochrome *c*, determined spectrophotometrically, was used as a measure of POR activity in membrane fractions.

Fluorogenic Probe Selection and Enzyme Kinetics. A panel of 12 fluorogenic substrates [ethoxyresorufin (ER), methoxyresorufin (MR), pentoxyresorufin (PR), benzyloxyresorufin (BR), AMMC, DBF, MFC, BQ, BFC, VIVID CYP2C9 Red, VIVID CYP2D6 Cyan, and VIVID CYP3A4 Red] was used in an initial screen to determine catalytic ability of the mouse P450s. Assays were performed in white 96-well plates (Thermo Labsystems, Basingtoke, UK) in a final volume of 200 μl containing 50 mM potassium phosphate buffer, pH 7.4, test substrate, 20 pmol of P450, and 125 μM NADPH. Reactions were initiated with the addition of the NADPH to the prewarmed plate. Substrate concentrations used were: DBF, 1 μM; ER, PR, MR, and BR, 2 μM; AMMC, 20 μM; MFC, 75 μM; BQ, 40 μM; BFC, 50 μM; VIVID

TABLE 2

Apparent kinetic parameters of the murine and human P450s coexpressed with human POR for a series of fluorescent probe substrates

Standard errors for K_m and V_{max} are to fit of the Michaelis-Menten curve.

P450	Organism	Substrate	K_m	V_{max}
			μM	
Cyp1a1	Mouse	ER	0.04 ± 0.002	12.5 ± 0.25[a]
Cyp1a2	Mouse	MR	0.03 ± 0.006	0.4 ± 0.002[a]
Cyp1b1	Mouse	ER	0.2 ± 0.01	1.5 ± 0.05[a]
Cyp2a4	Mouse	VIVID CYP3A4 Red	1.6 ± 0.35	0.4 ± 0.03[b]
Cyp2b20	Mouse	BR	0.2 ± 0.01	2.9 ± 0.07[a]
Cyp2c29	Mouse	VIVID CYP2C9 Red	0.7 ± 0.07	0.07 ± 0.002[b]
Cyp2d22	Mouse	VIVID CYP3A4 Red	1.2 ± 0.1	0.05 ± 0.003[b]
Cyp2e1	Mouse	VIVID CYP3A4 Red	1.7 ± 0.32	0.08 ± 0.006[b]
Cyp3a11	Mouse	DBF	0.5 ± 0.03	0.7 ± 0.01[b]
CYP2C9	Human	VIVID CYP2C9 Red	0.1 ± 0.002	0.5 ± 0.04[b]
CYP2D6	Human	AMMC	2.4 ± 0.7	0.4 ± 0.003[b]
CYP3A4	Human	DBF	0.1 ± 0.02	1.9 ± 0.01[b]

[a] Units: picomoles resorufin per minute per picomoles P450.
[b] Units: change in fluorescence per minute (arbitrary units).

CYP2D6 Cyan and VIVID CYP3A4 Red, 15 μM; and VIVID CYP2C9 Red, 10 μM. Reactions were measured in real time (10-s intervals) for 2 to 3 min at the published excitation and emission wavelengths for each probe using a Fluoroskan Ascent FL plate reading fluorimeter (Labsystems).

The probe substrates that gave the highest turnovers in the screening assay were used to determine the apparent kinetic parameters for the respective P450. Assays were performed under conditions of linearity for time and protein (data not shown) using the same buffer/NADPH conditions described in the previous paragraph, with the following concentrations of P450 and substrates (10 concentration points per determination): Cyp1a1 (0.25 pmol/well) and ER (0–1 μM); Cyp1a2 (5 pmol/well) and ER (0–0.5 μM); Cyp1B1 (2 pmol/well) and ER (0–1.2 μM); Cyp2b20 (1 pmol/well) and BR (0–1.25 μM); Cyp2a4 (1.5 pmol/well) and VIVID CYP3A4 Red (0–7.5 μM); Cyp2c29 (5 pmol/well) and VIVID CYP2C9 Red (0–20 μM); CYP2C9 (7.5 pmol/well) and VIVID CYP2C9 Red (0–15 μM); Cyp2d22 (3 pmol/well) and VIVID CYP3A4 Red (0–5 μM); CYP2D6 (15 pmol/well) and AMMC (0–50 μM); Cyp2e1 (20 pmol/well) and VIVID CYPA4 Red (0–7.5 μM); Cyp3a11 (5 pmol/well) and DBF (0–3 μM); and CYP3A4 (5 pmol/well) and DBF (0–0.5 μM). For ER and MR assays, turnover rates were calculated using an authentic resorufin standard curve, whereas, for all other probes, rates were calculated as average change in fluorescence per minute as calculated by the Fluoroskan Ascent software. Assays were run in duplicate, and in all cases variability was less than 10%. The data generated were analyzed by nonlinear regression using the Michaelis-Menten equation (GraFit version 5; Erithacus Software, Horley, UK).

Ligand IC_{50} Determination. For each IC_{50} determination, 386 μl of an enzyme/substrate master-mix containing 50 mM potassium phosphate, pH 7.4, probe substrate at a concentration equivalent to the K_m calculated for the P450 isoform being tested, and X pmol of P450 (see above for specific details) were added to well A1 of a white 96-well plate. Test ligand (4 μl) dissolved in methanol (for the majority of ligands) or dimethyl sulfoxide was then added. Whichever solvent the test ligand was dissolved in was then added to the remaining enzyme/substrate master-mix to give a final concentration of solvent of 1%, and 195 μl of this solution was added to wells A2–A12. Well A1 was thoroughly mixed and 195 μl removed serially diluted to well A11, and the excess 195 μl was discarded. Well A12 acted as a "no-ligand" control. Determinations were run in duplicate for 2 min measuring every 10 sec, allowing four compounds to be tested per plate. Plates were preincubated at 37°C for 3 min and reactions initiated with NADPH as before. Test compounds were used at a final concentration range of 0 to 100 μM. IC_{50} curves were plotted and values calculated using GraFit version 5. The concentration of solvent used was identical for both control and inhibited reactions, caused negligible inhibition of enzyme activities, and did not effect the IC50 values generated.

Results

P450 Cloning and Coexpression. To characterize ligand specificity of the 9 murine P450s, the cDNAs were modified for optimum expression in *E. coli* by the addition of an OmpA leader sequence. Coexpression with human POR, which has a 91% identity to murine POR, allowed production of bacterial membranes containing a functional monooxygenase system. Levels of whole cell expression varied dramatically among isoforms, ranging from approximately 50 nM for Cyp1b1 to 1400 nM for Cyp2e1. Representative P450 spectra and relative expression levels are detailed in Fig. 1. All isoforms were reasonably stable during P450 measurement, with the exception of Cyp1a1, which readily formed P420. Notably, Cyp2e1 was very slow to fully reduce, taking up to 20 min to reach saturation. POR expression levels were quantified by measuring NADPH-dependent cytochrome *c* reduction, where activities typically ranged from 200 to 500 nmol cytochrome *c* reduced per min/mg protein.

Fluorogenic Probe Selection. To assess enzyme activities and determine suitable fluorogenic probes for each P450 isoform, the enzymes were initially screened with the alkoxyresorufins ER, MR, PR, and BR. Cyp1b1 was the most promiscuous, capable of metabolizing all 4 analogs followed by Cyp1a1, which metabolized ER, MR, and BR. Cyp1a2 showed activity toward only ER and MR, whereas Cyp2b20 turned over PR and BR. Of the remaining isoforms, only Cyp2a4 (ER) and Cyp2c29 (MR) showed any activity toward the alkoxyresorufins, although the turnover was not sufficient for use as a substrate probe. The remainder of the isoforms were further screened with the alternate probes (AMMC, DBF, MFC, BQ, and BFC) where Cyp2c29 showed low level activity toward MFC and Cyp3a11 proved to efficiently metabolize DBF (also BFC). Interestingly, Cyp2d22 did not metabolize the CYP2D6 prototypical fluorogenic substrate AMMC. Finally, following screening with VIVID substrates, VIVID CYP3A4 Red was found to be a suitable substrate for Cyp2a4, Cyp2e1, and Cyp2d22, whereas Cyp2c29 was found to metabolize VIVID CYP2C9 Red. Again, Cyp2d22 did not efficiently turn over the CYP2D6 substrate VIVID CYP2D6 Cyan. The probes that exhibited the most efficient turnovers were used to determine the apparent kinetic parameters for each enzyme. Assays were performed under conditions of linearity for both time and protein (data not shown) and followed simple Michaelis-Menten kinetics. As shown in Table 2, the majority of enzymes exhibited nanomolar K_m values for their respective substrates. CYP3A4 and CYP2C9 metabolized DBF and VIVID CYP2C9 Red, respectively, with a greater apparent intrinsic clearance than their respective murine counterparts. Because CYP2D6 was not capable of metabolizing VIVID CYP3A4 Red, the kinetic parameters of the known CYP2D6 fluorogenic probe, AMMC, were determined instead.

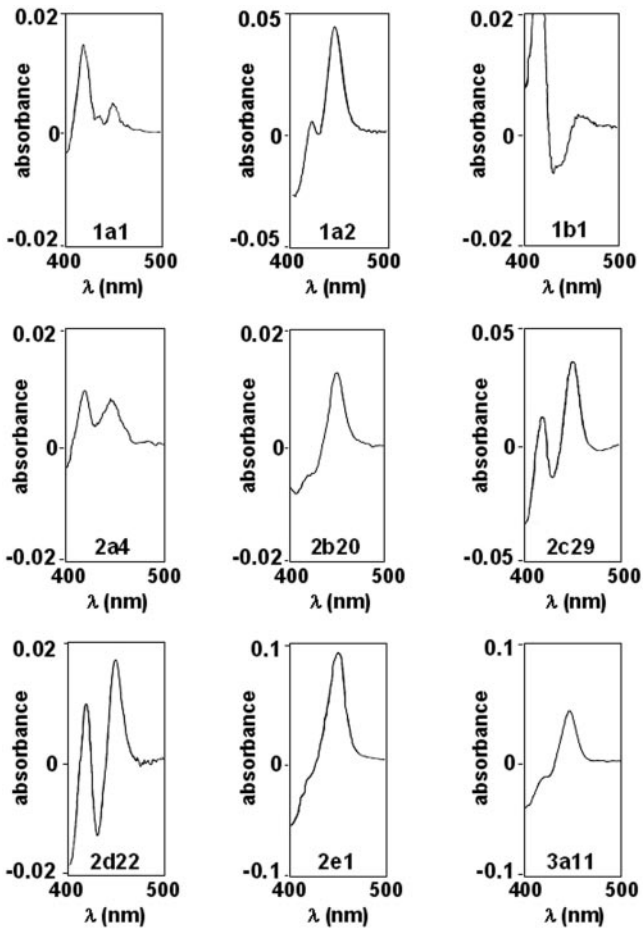

FIG. 1. Fe^{2+}-CO versus Fe^{2+} difference spectrum determined from *E. coli* cells coexpressing murine P450s and human POR. Spectra were determined from 0.5 to 1 ml of culture resuspended in 100 mM Tris-Cl, pH 7.4, containing 20% (v/v) glycerol, 10 mM CHAPS, and 1 mM EDTA. Expression levels were Cyp1a1, 80 nM; Cyp1a2, 1100 nM; Cyp1b1, 50 nM; Cyp2a4, 150 nM; Cyp2b20, 450 nM; Cyp2c29, 550 nM; Cyp2d22, 450 nM; Cyp2e1, 1400 nM; and Cyp3a11, 1100 nM.

Ligand IC_{50} Determination. With the aim of obtaining a ligand profile and thus a potential substrate and inhibitor profile for each murine isoform, a wide range of structurally diverse compounds were screened (Table 3) for inhibitory potential. The IC_{50} data generated for each P450 isoform are detailed in Table 4 and ranged from examples of very strong inhibition [e.g., Cyp2a4/methoxychlor and Cyp1a1/quercetin (IC_{50}: 10 nM)] to no inhibition (e.g., Cyp2e1/dihydroergotamine) and also activation (e.g., Cyp2d22/cholesterol). As a control, known benchmark substrates/inhibitors of the human P450s (e.g., CYP2C9/diclofenac, CYP2D6/quinidine, and CYP3A4/midazolam) gave IC_{50} values within the expected ranges.

In general, the "natural compounds" were found to strongly inhibit Cyp1a1, Cyp1a2, Cyp1b1, and Cyp2b20 and, to a lesser extent, Cyp2a4 and Cyp2c29. Cyp2d22 and -3a11 followed a similar pattern but were not inhibited by either dihydroergotamine or 5-methoxyindole. Cyp2e1 was the exception to this, showing inhibition only with quercetin. The three human P450s were inhibited by all the natural product compounds, with CYP2C9 activity inhibited to the greatest extent. With respect to the pesticide compound set, warfarin did not markedly inhibit any P450 other than CYP2C9 (IC_{50}: 3.5 μM) and Cyp2b20 (IC_{50}: 30.7 μM), whereas glyphosate was either noninhibitory or caused activation of the substrate metabolism. P450s 2b20, 2c29, 2C9, 2d22, 2e1, 3a11, and 3A4 were either weakly inhibited or not inhibited by isoproturon, whereas the remainder of the isoforms exhibited IC_{50}s of <11 μM. Surprisingly, the comparatively large molecule ivermectin inhibited all of the P450 isoforms with the exception of Cyp1a2, giving IC_{50} values in the range of 0.2 to 52.8 μM. The insecticides methoxychlor and cypermethrin were potent inhibitors of P450s 1a1, 2a4, 2b20, 2c29, and 2C9 but did not, however, inhibit Cyp1a2.

The "endogenous compounds" set produced a broad range of inhibition profiles. With the exception of Cyp2e1 and, to a lesser extent, CYP2D6, retinoic acid efficiently inhibited the metabolic capability of all P450 isoforms (IC_{50} values ranging from 1.3–16.6 μM). Although vitamin D3 was noninhibitory for the majority of murine enzymes, it significantly inhibited the activity of all three human P450s. The neurotransmitter dopamine significantly inhibited only Cyp1a2, Cyp1b1, and CYP2C9-mediated metabolism, whereas the bile acid lithocholic acid was capable of inhibiting all P450s, except CYP2D6, with varying degrees of potency. The murine testosterone hydroxylase Cyp2a4 bound testosterone with the lowest IC_{50} of 2.1 μM followed by CYP3A4 (IC_{50}: 5 μM) and Cyp2d22 (IC_{50}: 8.1 μM), whereas the other known testosterone hydroxylases, Cyp2b20 and Cyp3a11, showed 15- to 20-fold higher IC_{50}s. With respect to both species, cholesterol was a weak inhibitor, with Cyp2b20 giving the lowest IC_{50} of 29.6 μM.

The "drugs" compound set also produced a variety of inhibition patterns. Midazolam was noninhibitory toward P450 1a2, 2d22, and 2e1 activities but showed reasonably strong inhibition with the other enzymes ($IC_{50} < 18$ μM). In contrast to ivermectin, only Cyp2d22, CYP2C9, and CYP3A4 were able to bind erythromycin, a similarly large molecule. Ketoconazole was a potent inhibitor of all enzymes except Cyp2d22 and Cyp2e1. Only CYP2C9 was significantly inhibited by the acidic compound diclofenac, with Cyp2c29 exhibiting approximately 36-fold weaker inhibition (IC_{50}: 0.7 versus 25 μM). Tamoxifen and nifedipine were found to be universal inhibitors with reasonable potency (IC_{50} <60 or <40 μM, respectively). Interestingly, quinidine, a very potent inhibitor of human CYP2D6, did not strongly inhibit the activity of the mouse ortholog Cyp2d22 (IC_{50}: 85.8 μM).

Taking a broader view of the IC_{50} data, CYP2C9 and Cyp1a1 proved to be the most promiscuous enzymes, with only 3.2 and 12.9% of compounds tested being noninhibitors, respectively (Table 4). Cyp2e1 lay at the opposite end of the spectrum, where almost 50% of compounds were noninhibitory and no single compound exhibited particularly strong inhibition. Most surprisingly, Cyp2d22 was the enzyme that most frequently exhibited cooperative behavior, with 23% of the ligands causing substrate activation. Furthermore, this enzyme was also able to bind the three largest ligands, dihydroergotamine, ivermectin, and erythromycin, potentially indicating a larger active site than the other murine enzymes.

Correlation Analysis. When the correlation coefficients (cc) of the IC_{50} data were calculated (Table 5), the ligand bindings of Cyp1a1 and Cyp1b1 were most closely related (cc: 0.88). Strikingly, Cyp2d22 shows virtually no significant correlation with any murine P450 with the exception of Cyp2e1 and, to a lesser extent, Cyp1b1. Furthermore, Cyp2d22 shows an inversely correlated relationship with Cyp2c29. The remaining murine and human P450s, with the exception of Cyp1a2, demonstrated significant interenzyme binding correlations. A very marked correlation was observed between Cyp3a11 and CYP3A4 (cc: 0.81) and Cyp2c29 and CYP2C9 (cc: 0.77), whereas there was no correlation between Cyp2d22 and CYP2D6 inhibition.

No relationship between correlation coefficients and protein identity was observed, even within members of the same families (Table 6). For example, Cyp1a1 and Cyp1a2 have a high degree of sequence identity with P450s 1b1, 2b20, 2c29, and 2e1; however, their IC_{50}

TABLE 3

Chemical structures of test ligands used in IC_{50} screen

Natural Compounds			
Dihydroergotamine	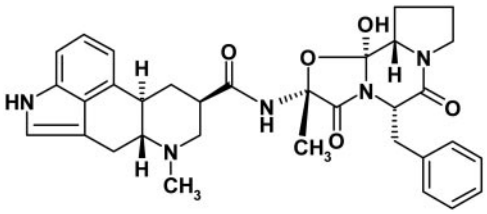	5-Methoxyindole	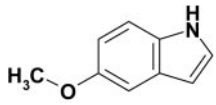
8-MOP	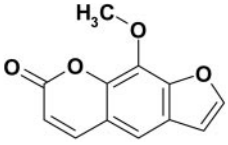	Quercetin	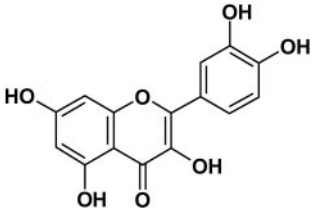
Resveratrol	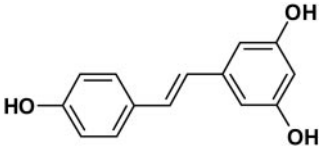	Daidzein	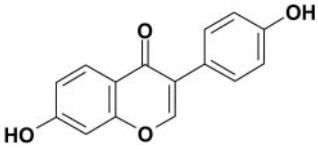
Pesticides			
Glyphosate	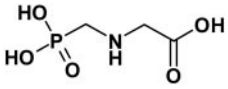	Warfarin	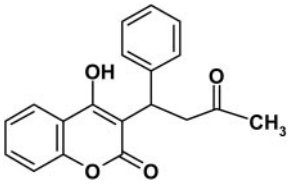
Isoproturon	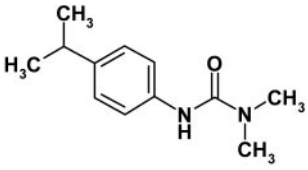	Methoxychlor	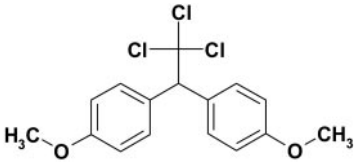
Cypermethrin	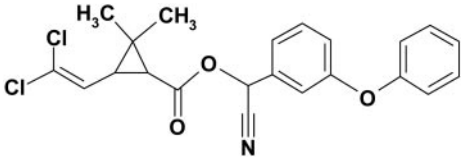	Ivermectin	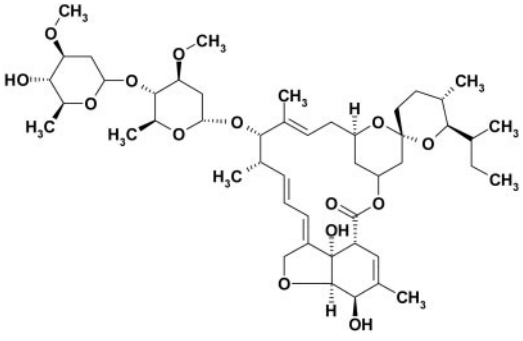
Endogenous Compounds			
Dopamine	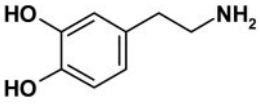	Cholesterol	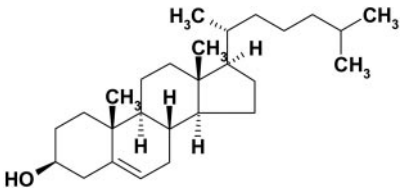

(*continued*)

TABLE 3—*Continued.*

Retinoic Acid	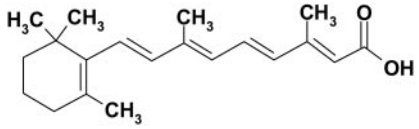	Testosterone	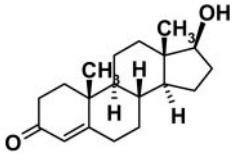
Vitamin D3	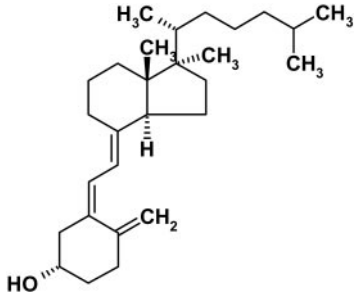	Lithocholic acid	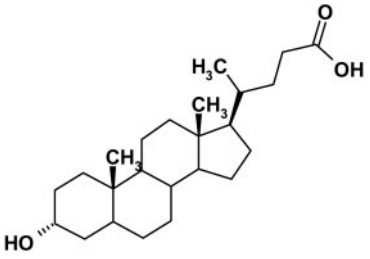
Drugs			
Midazolam	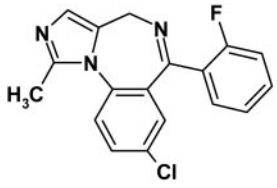	Cyclophosphamide	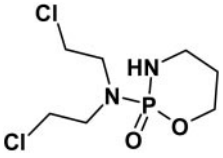
Erythromycin	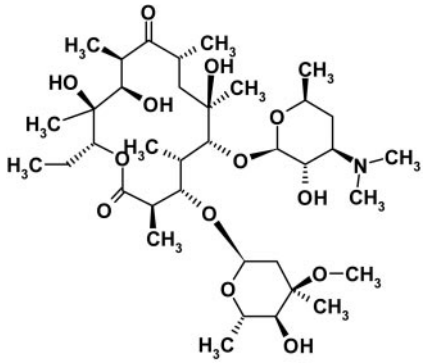	Tamoxifen	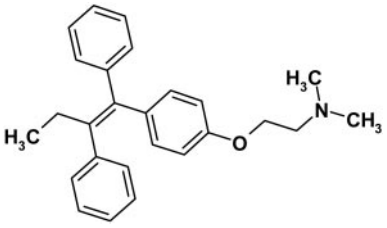
Dextromethorphan	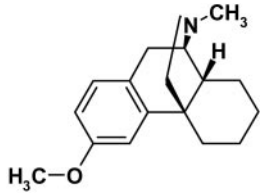	*S*-Mephenytoin	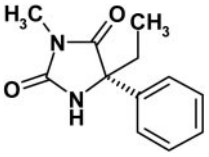
Ketoconazole	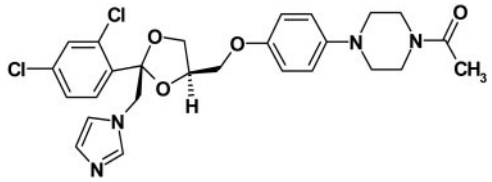	Quinidine	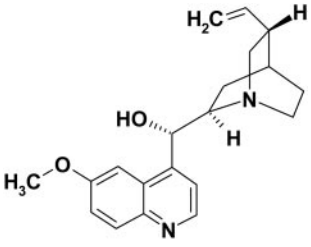
Caffeine	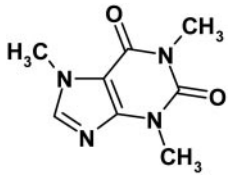	Omeprazole	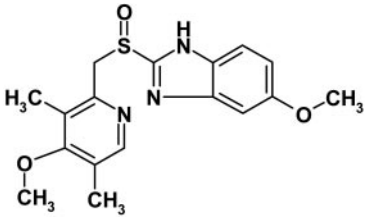

(*continued*)

TABLE 3—*Continued.*

Verapamil	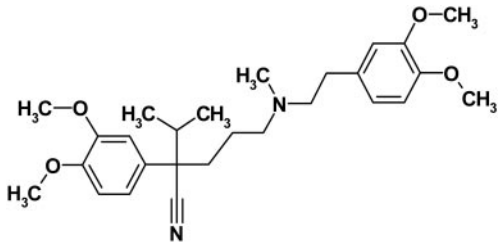	Nifedipine	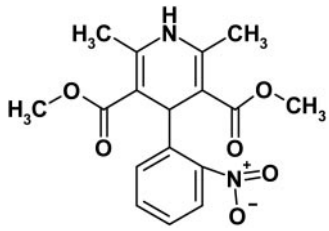
Diclofenac	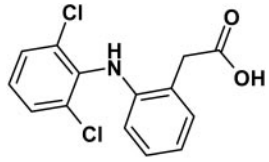		

8-MOP, methoxypsoralen.

TABLE 4

IC_{50} data for 31 test compounds with nine murine and three human P450 isoforms

IC_{50} values are in μM, with values prefixed with ≈ indicating IC_{50} values predicted by GraFit version 5 because of values being higher than the highest concentration of inhibitor used. Standard deviation of IC_{50} values in all cases was <10%.

Compound	Cyp1a1	Cyp1a2	Cyp1b1	Cyp2a4	Cyp2b20	Cyp2c29	Cyp2d22	Cyp2e1	Cyp3a11	CYP2C9	CYP2D6	CYP3A4
Dihydroergotamine	8.7	NI	10.5	70.8	7.3	16.9	1.3	NI	0.21	0.39	9.9	0.02
8-MOP	0.32	0.27	0.20	0.11	2.3	9.8	NI	105.8	76.7	6.7	28.4	22.2
Resveratrol	0.32	1.5	0.78	37.4	5.7	5.6	13.9	≈320	20.2	2.3	9.8	6.8
5-Methoxyindole	1.5	2.0	1.57	12.6	2.8	28.5	NI	96.4	NI	5.4	41.8	25.9
Quercetin	0.01	0.02	0.02	14.0	1.4	0.99	10.7	10.4	2.7	1.5	9.1	2.7
Daidzein	1.2	15.0	2.16	≈234	NI	1.8	34.8	≈280	≈192	2.7	36.5	14.8
Glyphosate	NI	NI	NI	NI	ACT	ACT	ACT	NI	NI	NI	NI	NI
Isoproturon	5.2	0.72	8.1	11.0	NI	167.7	NI	NI	NI	49.0	≈550	>1000
Cypermethrin	0.45	≈600	100.1	3.4	1.2	1.8	ACT	45.2	8.1	1.8	25.7	5.6
Warfarin	151.5	NI	NI	≈550	30.7	130.3	NI	NI	NI	3.5	≈310	56.6
Ivermectin	4.5	ACT	0.24	24.1	16.04	11.6	0.77	45.6	52.8	3.8	7.9	39.2
Methoxychlor	0.36	NI	9.5	0.01	0.08	0.54	ACT	90.9	6.8	1.8	≈190	10.8
Dopamine	115.8	23.4	40.2	NI	NI	≈500	NI	≈230	NI	50.0	≈450	≈950
Retinoic acid	1.3	2.8	4.4	1.7	1.7	7.0	16.6	NI	2.7	5.8	51.6	0.79
Vitamin D3	NI	NI	NI	NI	NI	119.3	NI	NI	≈300	4.0	8.7	5.4
Cholesterol	94.4	NI	NI	90.6	29.6	NI	ACT	49.8	ACT	≈180	NI	≈225
Testosterone	16.3	NI	81.8	2.1	34.6	40.2	8.1	NI	41.5	17.6	NI	5.0
Lithocholic acid	10.3	58.8	43.7	78.7	20.4	154.7	107.3	90.5	18.1	8.6	NI	6.8
Midazolam	5.7	NI	17.6	6.3	10.0	7.4	NI	NI	2.4	7.2	54.0	0.027
Erythromycin	NI	NI	NI	NI	NI	≈300	59.6	ACT	NI	70.3	NI	4.7
Dextromethorphan	100.9	NI	108.5	141.0	21.3	NI	ACT	≈400	NI	33.9	0.89	12.2
Ketoconazole	0.58	4.82	0.10	1.1	0.04	3.4	NI	NI	0.02	0.007	0.85	0.005
Caffeine	≈220	86.7	156.9	≈370	NI	NI	NI	NI	NI	61.9	NI	>1000
Verapamil	8.8	170.0	26.6	≈240	73.7	≈500	98.1	NI	38.2	15.9	12.7	2.1
Diclofenac	144.8	NI	≈210	≈280	154.1	25.0	NI	NI	NI	0.74	NI	>1000
Cyclophosphamide	≈170	≈210	NI	87.1	NI	NI	NI	NI	NI	60.7	NI	>1000
Tamoxifen	1.8	20.9	15.2	43.6	0.86	17.2	ACT 46.2	58.5	28.0	5.10	5.2	1.6
S-Mephenytoin	NI	NI	≈190	11.5	≈220	≈170	NI	≈240	≈560	56.6	NI	≈170
Quinidine	26.1	NI	96.8	NI	81.3	≈320	85.8	NI	≈480	32.7	0.01	5.8
Omeprazole	7.5	≈190	16.4	NI	50.8	NI	NI	NI	61.7	4.8	16.8	4.5
Nifedipine	2.7	17.9	4.7	15.3	0.80	37.4	ACT	25.0	6.3	0.30	39.9	1.1

8-MOP, methoxypsoralen; NI, not inhibitory; ACT, compound caused activation of probe substrate.

correlation coefficients indicate that these enzymes are extremely different. Another striking example is that of CYP2D6 and Cyp2d22 which, although 77% identical at the protein level, exhibit no similarities in binding capacity.

Discussion

Identification of the specific P450 that conclusively mediates a particular pathway of metabolism or catabolism has been simplified in the last 15 to 20 years with the advent of recombinant DNA technology, which generated a molecular tool set for dissecting the roles of specific enzymes. This becomes particularly pertinent in animals such as the mouse, where P450 subfamilies contain up to 15 members that, by definition, will share close sequence identity and possibly similar substrate specificity. Furthermore, with the increasing prevalence of genetically modified mouse models for studying disease progression and possible treatments (e.g., Alzheimer's disease, Huntington's disease, and cancer) (Mangiarini et al., 1996; Johnson et al., 1997; Ishihara et al., 1999) and the generation of mice "humanized" for drug metabolizing enzymes (Dragin et al., 2007; van Herwaarden et al., 2007; Felmlee et al., 2008), it has now become imperative that the metabolism and disposition of potential drug treatments are investigated in these animals and the implications for human pharmacoki-

TABLE 5

Spearman's rank-order correlation coefficients for the IC_{50} values of nine murine and three human P450s

Spearman's rank order correlation coefficients were calculated using Statistica version 6, where a correlation of 1.00 indicates identical data, 0 nonidentical data, and a negative value an inverse correlation.

P450	Cyp1a1	Cyp1a2	Cyp1b1	Cyp2a4	Cyp2b20	Cyp2c29	Cyp2d22	Cyp2e1	Cyp3a11	CYP2C9	CYP2D6	CYP3A4
Cyp1a1	1.00	0.61	0.88	0.68	0.77	0.78	0.13	0.52	0.65	0.61	0.51	0.42
Cyp1a2		1.00	0.64	0.32	0.29	0.29	0.07	0.25	0.23	0.21	0.16	0.13
Cyp1b1			1.00	0.59	0.62	0.67	0.34	0.40	0.61	0.55	0.52	0.40
Cyp2a4				1.00	0.70	0.67	0.00	0.37	0.56	0.34	0.13	0.28
Cyp2b20					1.00	0.68	−0.1	0.54	0.71	0.64	0.49	0.59
Cyp2c29						1.00	−0.24	0.37	0.70	0.77	0.43	0.45
Cyp2d22							1.00	0.39	0.28	0.13	0.08	0.25
Cyp2e1								1.00	0.21	0.27	0.24	−0.03
Cyp3a11									1.00	0.66	0.43	0.81
CYP2C9										1.00	0.55	0.50
CYP2D6											1.00	0.47
CYP3A4												1.00

TABLE 6

Percentage identity between the protein sequences of nine murine and three human P450 isoforms

Protein alignments were carried out using an on-line ClustalW server (http://www.ch.embnet.org/index.html), and the results were exported into Jemboss Alignment Editor (http://emboss.sourceforge.net/Jemboss) and percentage identity calculated.

P450	Cyp1a1	Cyp1a2	Cyp1b1	Cyp2a4	Cyp2b20	Cyp2c29	Cyp2d22	Cyp2e1	Cyp3a11	CYP2C9	CYP2D6	CYP3A4
Cyp1a1	100	71.3	38.0	32.2	29.9	30.3	29.7	30.9	22.5	30.7	29.3	23.1
Cyp1a2		100	35.1	30.6	29.5	30.8	29.7	30.9	22.5	31.6	30.9	22.7
Cyp1b1			100	26.5	27.6	29.0	28.6	25.8	17.7	28.3	30.0	18.0
Cyp2a4				100	58.6	58.7	41.1	52.8	26.7	55.0	41.7	27.4
Cyp2b20					100	54.0	44.5	52.1	27.6	54.0	45.5	27.8
Cyp2c29						100	43.8	58.2	27.9	78.5	44.6	27.8
Cyp2d22							100	40.4	25.3	42.4	76.9	24.7
Cyp2e1								100	27.0	60.8	42.2	26.7
Cyp3a11									100	26.5	24.9	74.9
CYP2C9										100	44.2	27.1
CYP2D6											100	24.7
CYP3A4												100

netics assessed. The mouse is also heavily used as a toxicology model and, since many carcinogens and hepatotoxic compounds are required to be activated by P450s in order to exert their deleterious effects, it is essential to understand the function of mouse P450s in order to be able to extrapolate the results back to humans in a meaningful way.

Due to the problem of gene multiplicity masking the activities of the individual isoform, the most straightforward method of defining substrate specificity is by heterologous expression and subsequent characterization of individual P450s. We therefore used a previously developed strategy (Blake et al., 1996; Pritchard et al., 1997; Pritchard et al., 1998) that enabled the efficient coexpression of POR and nine murine P450s in *E. coli*. Rather than establishing individual assays for all the compounds, we established instead a fluorogenic assay for each murine P450 to determine the inhibitory potential of a set of test compounds, allowing us to compare inhibitory potencies of several test compounds. The range of readily available fluorogenic probe compounds enabled a substrate to be found for all the murine P450s tested in this study, resulting in an efficient and robust basis for inhibition screening. Surprisingly, the CYP3A4 specific substrate VIVID CYP3A4 Red proved to be a suitable probe for Cyp2d22, whereas the CYP2D6-specific probes VIVID CYP2D6 Cyan and AMMC were not metabolized. This "un-CYP2D6-like" behavior is supported by work carried out by Yu and Haining (2006), who suggest that Cyp2d22 is not the murine enzyme responsible for CYP2D6-like activity, behaving instead with a more "CYP3A4-like" tendency.

Four general sets of ligands were chosen for the inhibition screen—natural product compounds, pesticides, endogenous compounds, and common drugs—many of which are known to undergo P450-mediated metabolism. Analysis of the inhibition data has confirmed a major difference between Cyp2d22 and CYP2D6 ligand preference. Aside from this, some interesting similarities and differences between human and mouse P450 activity inhibition were noted. For example, resveratrol, quercetin, and daidzein strongly inhibited the Cyp1 family, data which are mirrored by experiments done with the human homologs (Obach, 2000; Chang et al., 2001; Roberts et al., 2004). Also, there were considerable similarities between the data generated for Cyp2a4 with literature values for CYP2A6 (Draper et al., 1997), whereas the well characterized CYP2C9 substrate warfarin showed 43-fold lower inhibition with Cyp2c29 than with CYP2C9. Other notable differences include the well known CYP2B6 substrate cyclophosphamide (Chang et al., 1993), demonstrating no inhibition of Cyp2b20 activity; the CYP3A4 substrate erythromycin, having no effect on Cyp3a11 activity, perhaps indicating a smaller or less flexible active site to CYP3A4; and methoxychlor, a known substrate of CYP1A2, CYP2B, and CYP2C9 (Stresser et al., 1996; Stresser and Kupfer, 1998), potently inhibiting Cyp2b20 and Cyp2c29 but having no effect on Cyp1a2. Broadly speaking, however, the Cyp2c29 and Cyp3a11 data correlated well with the human equivalents, although, on a compound-by-compound basis, human CYP2C9 and CYP3A4 tended to be more markedly inhibited than the mouse Cyp2c29 and Cyp3a11.

Although Cyp2d22 and CYP2D6 are considered orthologs, exhibiting 77% identity at the protein level, the vastly different inhibition profiles indicate that the active site of Cyp2d22 is most likely distinct from CYP2D6. Structure-based sequence alignment of the two proteins (Fig. 2) indicate that, although the residues which are key determinants of substrate specificity in CYP2D6, Glu216, and Asp301 (Paine et al., 2003) are conserved in Cyp2d22, two further residues,

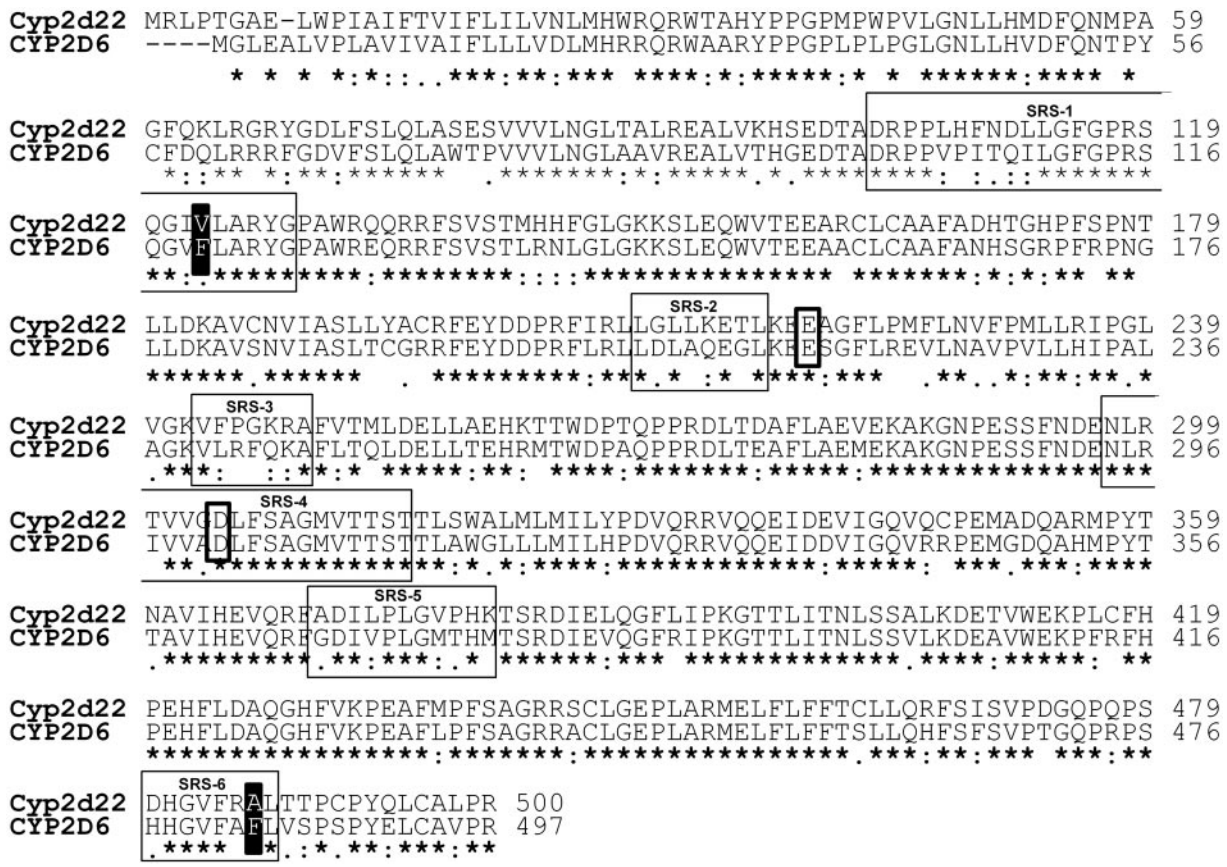

FIG. 2. Structure-based alignment of the amino acid sequences of Cyp2d22 and CYP2D6 proteins, indicating the structure recognition sites (SRS) (Gotoh, 1992) and key active site residues. Protein sequences of the two enzymes were analyzed using the EXPRESSO (3DCoffee) server (Armougom et al., 2006), which aligns sequences using structural information. Boxed residues correspond to Glu216 and Asp301 in CYP2D6, which are conserved in Cyp2d22, and shaded boxes indicate Phe120 and Phe483 in CYP2D6, which are not conserved in the mouse ortholog.

Phe120 and Phe483 (Smith et al., 1998; Flanagan et al., 2004), which also play crucial roles in CYP2D6 structure activity relationships, are not similarly conserved. Site-directed mutation of these residues in CYP2D6 results in altered substrate specificity and regioselectivity (Flanagan et al., 2004; McLaughlin et al., 2005), which may explain in part the striking differences observed between the two enzymes observed by our lab and others (Yu and Haining, 2006). Furthermore, there are several nonconservative amino acid substitutions in the SRS-2 and SRS-3 of Cyp2d22 as compared with CYP2D6, which may also contribute to the differing substrate specificity and inhibition profiles obtained. Perhaps the most surprising characteristic of Cyp2d22 observed in this study is its ability to exhibit heterotropic cooperativity as demonstrated by activation of substrate turnover (Table 5). This is suggestive of a fundamental mechanistic difference between Cyp2d22 and members of other mammalian 2D subfamilies. To date, there have been no conclusive reports of cooperative behavior in CYP2D enzymes, and this gives further weight to the theory that Cyp2d22 is "CYP3A4-like" (Yu and Haining, 2006). Given that Cyp2d22 is one of the most abundant Cyp2d isoforms in mouse liver (Choudhary et al., 2003; Jenkins et al., 2006), these unusual traits could lead to possible misinterpretation of mouse liver microsome metabolism data and have potential implications for pharmacokinetic studies.

One drawback in using inhibition screening to profile the active sites of particular P450s is that it is indicative of the binding capacity of the active site but does not differentiate between the types of inhibition occurring and, obviously, does not indicate whether a compound will be a substrate or not. For example, nifedipine inhibited all P450s tested with IC_{50}s of <40 μM; however, it was only metabolized by CYP3A4 and Cyp3a11 (data not shown). The data generated in this study were designed to be an initial step in the profiling of murine P450 substrate specificity and are currently being followed up with more extensive metabolism studies.

In summary, we have functionally coexpressed nine murine P450 enzymes (Cyp1a1, Cyp1a2, Cyp1b1, Cyp2a4, Cyp2b20, Cyp2c29, Cyp2d22, Cyp2e1, and Cyp3a11) with POR and identified and kinetically characterized a fluorogenic probe for each enzyme, which was then used to produce a self-consistent matrix of IC_{50} values for 31 compounds. We have used correlation analysis to compare the inhibition profiles of these nine enzymes with each other and also with three human P450s (CYP2C9, CYP2D6, and CYP3A4) and shown that, in general, with the exception of Cyp2d22, there is reasonable agreement in P450 inhibition profiles between murine and human P450 orthologs. Furthermore, we have demonstrated that Cyp2d22 is remarkably unlike CYP2D6, showing differences in metabolism, inhibition, and allosteric behavior, which could have wide-ranging implications for the interpretation of pharmacokinetic data.

References

Abu-Abed S, Dolle P, Metzger D, Beckett B, Chambon P, and Petkovich M (2001) The retinoic acid-metabolizing enzyme, CYP26A1, is essential for normal hindbrain patterning, vertebral identity, and development of posterior structures. *Genes Dev* **15:**226–240.

Armougom F, Moretti S, Poirot O, Audic S, Dumas P, Schaeli B, Keduas V, and Notredame C (2006) Expresso: automatic incorporation of structural information in multiple sequence alignments using 3D-Coffee. *Nucleic Acids Res* **34:**W604–608.

Blake JA, Pritchard M, Ding S, Smith GC, Burchell B, Wolf CR, and Friedberg T (1996) Coexpression of a human P450 (CYP3A4) and P450 reductase generates a highly functional monooxygenase system in Escherichia coli. *FEBS Lett* **397:**210–214.

Buters JT, Sakai S, Richter T, Pineau T, Alexander DL, Savas U, Doehmer J, Ward JM, Jefcoate

CR, and Gonzalez FJ (1999) Cytochrome P450 CYP1B1 determines susceptibility to 7, 12-dimethylbenz[a]anthracene-induced lymphomas. *Proc Natl Acad Sci U S A* **96:**1977–1982.
Chang TK, Chen J, and Lee WB (2001) Differential inhibition and inactivation of human CYP1 enzymes by trans-resveratrol: evidence for mechanism-based inactivation of CYP1A2. *J Pharmacol Exp Ther* **299:**874–882.
Chang TK, Weber GF, Crespi CL, and Waxman DJ (1993) Differential activation of cyclophosphamide and ifosphamide by cytochromes P-450 2B and 3A in human liver microsomes. *Cancer Res* **53:**5629–5637.
Choudhary D, Jansson I, Schenkman JB, Sarfarazi M, and Stoilov I (2003) Comparative expression profiling of 40 mouse cytochrome P450 genes in embryonic and adult tissues. *Arch Biochem Biophys* **414:**91–100.
Dalton TP, Dieter MZ, Matlib RS, Childs NL, Shertzer HG, Genter MB, and Nebert DW (2000) Targeted knockout of Cyp1a1 gene does not alter hepatic constitutive expression of other genes in the mouse [Ah] battery. *Biochem Biophys Res Commun* **267:**184–189.
Dragin N, Uno S, Wang B, Dalton TP, and Nebert DW (2007) Generation of 'humanized' hCYP1A1_1A2_Cyp1a1/1a2(−/−) mouse line. *Biochem Biophys Res Commun* **359:**635–642.
Draper AJ, Madan A, and Parkinson A (1997) Inhibition of coumarin 7-hydroxylase activity in human liver microsomes. *Arch Biochem Biophys* **341:**47–61.
Felmlee MA, Lon HK, Gonzalez FJ, and Yu AM (2008) Cytochrome P450 expression and regulation in CYP3A4/CYP2D6 double transgenic humanized mice. *Drug Metab Dispos* **36:**435–441.
Flanagan JU, Marechal JD, Ward R, Kemp CA, McLaughlin LA, Sutcliffe MJ, Roberts GC, Paine MJ, and Wolf CR (2004) Phe120 contributes to the regiospecificity of cytochrome P450 2D6: mutation leads to the formation of a novel dextromethorphan metabolite. *Biochem J* **380:**353–360.
Flanagan JU, McLaughlin LA, Paine MJ, Sutcliffe MJ, Roberts GC, and Wolf CR (2003) Role of conserved Asp293 of cytochrome P450 2C9 in substrate recognition and catalytic activity. *Biochem J* **370:**921–926.
Gotoh O (1992) Substrate recognition sites in cytochrome P450 family 2 (CYP2) proteins inferred from comparative analyses of amino acid and coding nucleotide sequences. *J Biol Chem* **267:**83–90.
Guengerich FP (2005) Human cytochrome P450 enzymes, in *Cytochrome P450, structure, mechanism and biochemistry* (de Montellano O ed), pp 377–530, Kluwer Academic/Plenum Publishers, New York.
Hasler JA (1999) Pharmacogenetics of cytochromes P450. *Mol Aspects Med* **20:**12–24, 25–137.
Henderson CJ, Otto DM, Carrie D, Magnuson MA, McLaren AW, Rosewell I, and Wolf CR (2003) Inactivation of the hepatic cytochrome P450 system by conditional deletion of hepatic cytochrome P450 reductase. *J Biol Chem* **278:**13480–13486.
Henderson CJ and Wolf CR (2003) Transgenic analysis of human drug-metabolizing enzymes: preclinical drug development and toxicology. *Mol Interv* **3:**331–343.
Ishibashi S, Schwarz M, Frykman PK, Herz J, and Russell DW (1996) Disruption of cholesterol 7alpha-hydroxylase gene in mice. I. Postnatal lethality reversed by bile acid and vitamin supplementation. *J Biol Chem* **271:**18017–18023.
Ishihara T, Hong M, Zhang B, Nakagawa Y, Lee MK, Trojanowski JQ, and Lee VM (1999) Age-dependent emergence and progression of a tauopathy in transgenic mice overexpressing the shortest human tau isoform. *Neuron* **24:**751–762.
Jenkins RE, Kitteringham NR, Hunter CL, Webb S, Hunt TJ, Elsby R, Watson RB, Williams D, Pennington SR, and Park BK (2006) Relative and absolute quantitative expression profiling of cytochromes P450 using isotope-coded affinity tags. *Proteomics* **6:**1934–1947.
Johnson L, Greenbaum D, Cichowski K, Mercer K, Murphy E, Schmitt E, Bronson RT, Umanoff H, Edelmann W, Kucherlapati R, et al. (1997) K-ras is an essential gene in the mouse with partial functional overlap with N-ras. *Genes Dev* **11:**2468–2481.
Lee SS, Buters JT, Pineau T, Fernandez-Salguero P, and Gonzalez FJ (1996) Role of CYP2E1 in the hepatotoxicity of acetaminophen. *J Biol Chem* **271:**12063–12067.
Mangiarini L, Sathasivam K, Seller M, Cozens B, Harper A, Hetherington C, Lawton M, Trottier Y, Lehrach H, Davies SW, et al. (1996) Exon 1 of the HD gene with an expanded CAG repeat is sufficient to cause a progressive neurological phenotype in transgenic mice. *Cell* **87:**493–506.
McLaughlin LA, Paine MJ, Kemp CA, Marechal JD, Flanagan JU, Ward CJ, Sutcliffe MJ, Roberts GC and Wolf CR (2005) Why is quinidine an inhibitor of cytochrome P450 2D6? The role of key active site residues in quinidine binding. *J Biol Chem* **280:**38617–38624.
Miller WL (1988) Molecular biology of steroid hormone synthesis. *Endocr Rev* **9:**295–318.
Obach RS (2000) Inhibition of human cytochrome P450 enzymes by constituents of St. John's Wort, an herbal preparation used in the treatment of depression. *J Pharmacol Exp Ther* **294:**88–95.
Otto DM, Henderson CJ, Carrie D, Davey M, Gundersen TE, Blomhoff R, Adams RH, Tickle C, and Wolf CR (2003) Identification of novel roles of the cytochrome P450 system in early embryogenesis: effects on vasculogenesis and retinoic acid homeostasis. *Mol Cell Biol* **23:**6103–6116.
Paine MJ, McLaughlin LA, Flanagan JU, Kemp CA, Sutcliffe MJ, Roberts GC, and Wolf CR (2003) Residues glutamate 216 and aspartate 301 are key determinants of substrate specificity and product regioselectivity in cytochrome P450 2D6. *J Biol Chem* **278:**4021–4027.
Pineau T, Fernandez-Salguero P, Lee SS, McPhail T, Ward JM, and Gonzalez FJ (1995) Neonatal lethality associated with respiratory distress in mice lacking cytochrome P450 1A2. *Proc Natl Acad Sci U S A* **92:**5134–5138.
Pritchard MP, Glancey MJ, Blake JA, Gilham DE, Burchell B, Wolf CR, and Friedberg T (1998) Functional co-expression of CYP2D6 and human NADPH-cytochrome P450 reductase in Escherichia coli. *Pharmacogenetics* **8:**33–42.
Pritchard MP, Ossetian R, Li DN, Henderson CJ, Burchell B, Wolf CR, and Friedberg T (1997) A general strategy for the expression of recombinant human cytochrome P450s in Escherichia coli using bacterial signal peptides: expression of CYP3A4, CYP2A6, and CYP2E1. *Arch Biochem Biophys* **345:**342–354.
Roberts DW, Doerge DR, Churchwell MI, Gamboa da Costa G, Marques MM, and Tolleson WH (2004) Inhibition of extrahepatic human cytochromes P450 1A1 and 1B1 by metabolism of isoflavones found in Trifolium pratense (red clover). *J Agric Food Chem* **52:**6623–6632.
Smith G, Modi S, Pillai I, Lian LY, Sutcliffe MJ, Pritchard MP, Friedberg T, Roberts GC, and Wolf CR (1998) Determinants of the substrate specificity of human cytochrome P-450 CYP2D6: design and construction of a mutant with testosterone hydroxylase activity. *Biochem J* **331:**783–792.
Stresser DM, Dehal SS, and Kupfer D (1996) Ring hydroxylation of [o-3H]methoxychlor as a probe for liver microsomal CYP2B activity: potential for in vivo CYP2B assay. *Anal Biochem* **233:**100–107.
Stresser DM and Kupfer D (1998) Human cytochrome P450-catalyzed conversion of the proestrogenic pesticide methoxychlor into an estrogen. Role of CYP2C19 and CYP1A2 in O-demethylation. *Drug Metab Dispos* **26:**868–874.
van Herwaarden AE, Wagenaar E, van der Kruijssen CM, van Waterschoot RA, Smit JW, Song JY, van der Valk MA, van Tellingen O, van der Hoorn JW, Rosing H, et al. (2007) Knockout of cytochrome P450 3A yields new mouse models for understanding xenobiotic metabolism. *J Clin Invest* **117:**3583–3592.
Wu L, Gu J, Weng Y, Kluetzman K, Swiatek P, Behr M, Zhang QY, Zhuo X, Xie Q, and Ding X (2003) Conditional knockout of the mouse NADPH-cytochrome P450 reductase gene. *Genesis* **36:**177–181.
Yu AM and Haining RL (2006) Expression, purification, and characterization of mouse CYP2d22. *Drug Metab Dispos* **34:**1167–1174.

Address correspondence to: Dr. Colin J. Henderson, Biomedical Research Centre, University of Dundee, Ninewells Hospital and Medical School, Dundee DD1 9SY, UK. E-mail: c.j.henderson@dundee.ac.uk